Reference: *Biol. Bull.* **233:** 000–000. (December 2017)

Sphingolipid Metabolism of a Sea Anemone Is Altered by the Presence of Dinoflagellate Symbionts

SHEILA A. KITCHEN*, ANGELA Z. POOLE†, AND VIRGINIA M. WEIS

Department of Integrative Biology, Oregon State University, Corvallis, Oregon 97331

Abstract. In host-microbe interactions, signaling lipids function in interpartner communication during both the establishment and maintenance of associations. Previous evidence suggests that sphingolipids play a role in the mutualistic cnidarian-*Symbiodinium* symbiosis. Exogenously applied sphingolipids have been shown to alter this partnership, though endogenous host regulation of sphingolipids by the sphingosine rheostat under different symbiotic conditions has not been characterized. The rheostat regulates levels of pro-survival sphingosine-1-phosphate (S1P) and pro-apoptotic sphingosine (Sph) through catalytic activities of sphingosine kinase (SPHK) and S1P phosphatase (SGPP). The role of the rheostat in recognition and establishment of cnidarian-*Symbiodinium* symbiosis was investigated in the sea anemone *Aiptasia pallida* by measuring gene expression, protein levels, and sphingolipid metabolites in symbiotic, aposymbiotic, and newly recolonized anemones. Comparison of two host populations showed that symbiotic animals from one population had lower *SGPP* gene expression and Sph lipid concentrations compared to aposymbiotic animals, while the other population had higher S1P concentrations than their aposymbiotic counterparts. In both populations, the host rheostat trended toward host cell survival in the presence of symbionts. Furthermore, upregulation of both rheostat enzymes on the first day of host recolonization by symbionts suggests a role for the rheostat in host-symbiont recognition during symbiosis onset. Collectively, these data suggest a regulatory role of sphingolipid signaling in cnidarian-*Symbiodinium* symbiosis and symbiont uptake.

Received 2 May 2017; Accepted 6 November 2017; Published online 31 January 2018.

* To whom correspondence should be addressed. E-mail: kitchens.osu@gmail.com. Present address: Department of Biology, Pennsylvania State University, 208 Mueller Laboratory, University Park, Pennsylvania 16802.

† Present address: Department of Biology, Berry College, 2277 Martha Berry Highway Northwest, Mount Berry, Georgia 30149.

Abbreviations: C_t, cycle threshold; GMP, Gisele Muller-Parker population; LPS, lipopolysaccharide; MAMP, microbe-associated molecular pattern; NSL, no symbionts + light treatment group; qPCR, quantitative polymerase chain reaction; rt, room temperature; S1P, sphingosine-1-phosphate; SD, symbionts + dark treatment group; SGPP, sphingosine-1-phosphate phosphatase; SL, symbionts + light treatment group; Sph, sphingosine; SPHK, sphingosine kinase; VWA, Weis Lab population A.

Introduction

Sphingolipids are a family of membrane lipids that provide cell structure and act as signaling molecules that mediate host-microbe interactions (Heung *et al.*, 2006). The biological outcomes of sphingolipid signaling are numerous, including cell proliferation, apoptosis, inflammation, and pathogenesis (Maceyka *et al.*, 2002). These consequences are determined in part by the relative amounts of the bioactive sphingolipids sphingosine (Sph) and sphingosine-1-phosphate (S1P), which play pivotal roles in determining cell fate and host-microbe partnerships through the coupled enzymatic activities of sphingosine kinase (SPHK) and sphingosine-1-phosphate phosphatase (SGPP), collectively referred to as the sphingosine rheostat (Fig. 1; Cuvillier *et al.*, 1996). Under normal conditions in tissues, S1P is maintained at a constitutively low level through the enzymatic balance of sphingolipid generation and breakdown (Fig. 1; Schwab *et al.*, 2005; Chan and Pitson, 2013). However, elevations in cellular S1P promote cell survival and proliferation in numerous ways (reviewed by Olivera and Spiegel, 2001) and can have pleiotropic actions through the initiation of intracellular signaling cascades (Olivera *et al.*, 2003) and/or inside-out signaling through receptor-mediated activation of downstream effectors *via* S1P receptors ($S1PR_{1–5}$; Fig. 1; An *et al.*, 1997). In contrast, the reversible dephosphorylation of S1P to Sph by SGPP results in an accumulation of Sph and its precursor ceramide that drives pro-apoptotic activity within the cell and halts cell proliferation (Mandala *et al.*, 1998).

In addition to their important role in growth and survival, the rheostat lipids mediate phagocytosis of pathogenic and beneficial microbes (reviewed by Heung *et al.*, 2006). In the host,

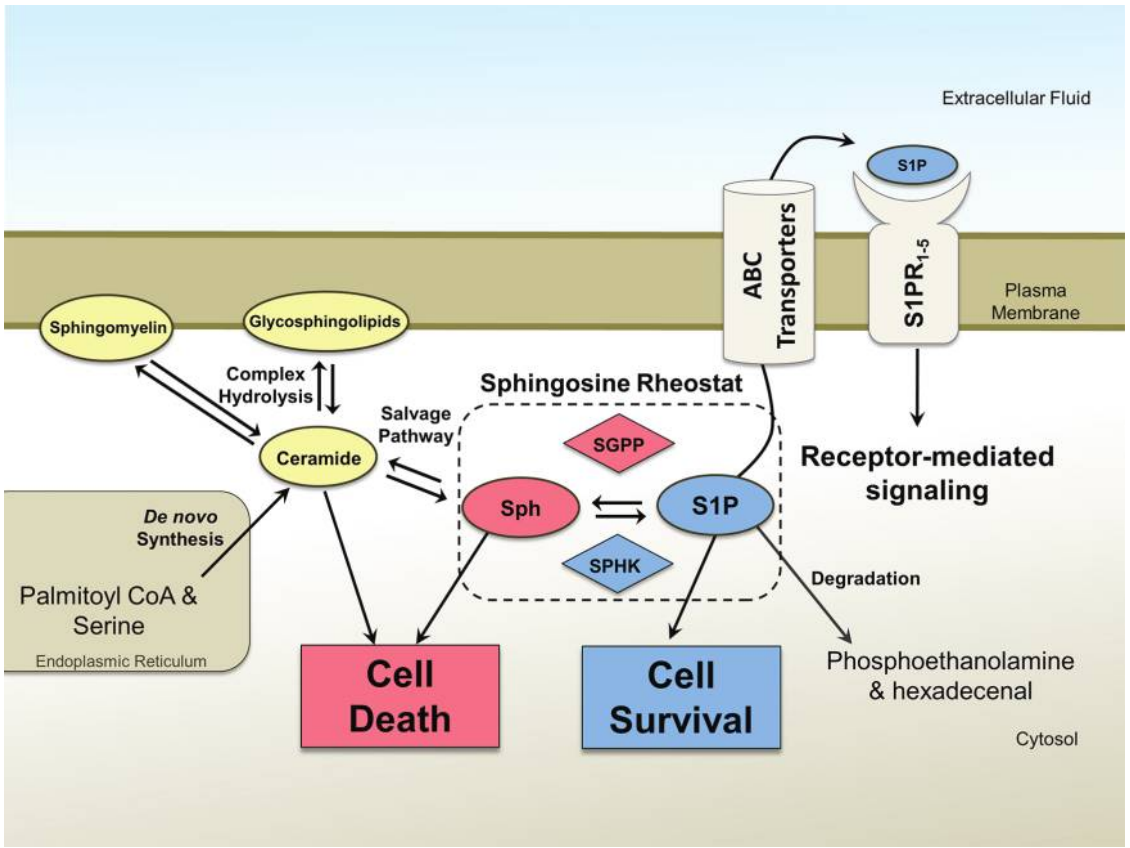

Figure 1. Schematic diagram of sphingolipid metabolism in a mammalian cell. *De novo* synthesis of sphingolipids takes place on the cytosolic surface of the endoplasmic reticulum (ER) and ER-associated membranes. The lipid intermediate ceramide is then incorporated into complex sphingolipids such as sphingomyelin in the Golgi apparatus and trafficked to the plasma membrane. Catabolism of ceramide releases the bioactive lipid sphingosine (Sph), and both contribute to activation of pro-apoptotic cellular cascades. Phosphorylation of Sph by sphingosine kinase (SPHK) produces the potent signaler sphingosine-1-phosphate (S1P), with extra- and intracellular signaling targets. Extracellular S1P is translocated by adenosine triphosphate-binding cassette (ABC) transporters and is bound by substrate-specific G-protein-coupled S1P receptors 1–5. Elevated cytosolic S1P enhances cell survival and proliferation. S1P can be dephosphorylated by S1P phosphatase (SGPP) or irreversibly degraded into phosphoethanolamine and hexadecenal. The enzymatic interconversion of S1P and Sph is known as the sphingosine rheostat (dashed box). Sphingolipids (ovals): Sph (red) = sphingosine, S1P (blue) = sphingosine-1-phosphate, ceramide, sphingomyelin, glycosphingolipids; enzymes (diamonds): SPHK 1 (blue) = sphingosine kinase, SGPP (red) = sphingosine-1-phosphate phosphatase.

sphingolipids are part of a rapid innate immune response to non-self molecules (Cinque *et al.*, 2003; Rivera *et al.*, 2008). For example, when specific cytokines or microbe-associated molecular patterns (MAMPs) bind to host receptors, SPHK is activated through an unknown mechanism, moves to plasma or phagosomal membranes, and produces S1P that ultimately causes intrinsic activation of transcription factors such as NF-κB, an immune response mediator (Xia *et al.*, 2002). Furthermore, inside-out S1P signaling is fundamental to immune cell migration, barrier integrity, and immune molecule expression (reviewed by Spiegel and Milstien, 2011). Microbes also use sphingolipids, produced endogenously or co-opted from their host, to evade the host immune response, enhance their survival and virulence, or disrupt host sphingolipid metabolism to modulate phagosomal maturation (Steinberg and Grinstein, 2008; Ali *et al.*, 2011; An *et al.*, 2014; Tafesse *et al.*, 2015). Therefore, the modulation of sphingolipids by the host, microbe, or both partners alters the ability of a microbe to colonize a host. The dynamic flux of these two signaling lipids is an important indicator of homeostatic imbalance, environmental perturbation, and, ultimately, cell fate of the host, which in turn dictate the survival of their microbial partners.

Initiation of the symbiosis between cnidarians, such as corals and sea anemones, and photosynthetic dinoflagellates in the genus *Symbiodinium* begins like many other host-microbe interactions, through phagocytosis of the algae into membrane-bound vesicles called symbiosomes (Davy *et al.*, 2012). This is the same pathway used for food acquisition and digestion and is a vital part of cnidarian innate immunity. Ultimately, the symbiosome compartment occupies a large volume of the

host cell (Davy *et al.*, 2012), requiring substantial investment in the remodeling and biosynthesis of host lipids (Garrett *et al.*, 2013). Differences in fatty-acid composition (Yamashiro *et al.*, 1999; Imbs *et al.*, 2010; Dunn *et al.*, 2012), endosymbiosis-specific lipid bodies (Simon and Rouser, 1967; Kellogg and Patton, 1983; Peng *et al.*, 2011; Chen *et al.*, 2015), and lipid profiles (Garrett *et al.*, 2013; Revel *et al.*, 2016) have been investigated in symbiotic cnidarians, but the role of host lipids in symbiont recognition and colonization is still unclear.

The cnidarian sphingosine rheostat model for symbiosis regulation was proposed following the discovery of the down-regulation of the gene *SGPP* in the symbiotic sea anemone *Anthopleura elegantissima* from a transcriptome study comparing symbiotic states (Rodriguez-Lanetty *et al.*, 2006). This transcriptional response to symbiosis suggested a shift in the rheostat toward increased S1P levels, which would correspond to increased host cell survival and symbiont proliferation. A subsequent study by Detournay and Weis (2011) explored the potential role of sphingolipid metabolism in cnidarian immunity by incubating the anemone *Aiptasia pallida* (also known as *Exaiptasia pallida*) (Grajales and Rodriguez, 2014) in the lipid metabolites Sph, S1P, and FTY720, an S1P agonist, followed by exposure to lipopolysaccharide (LPS), an immune-eliciting MAMP. Compared to controls, anemones without symbionts (aposymbiotic) incubated in S1P and FTY720, followed by LPS challenge, exhibited decreased levels of the cytotoxic nitric oxide (NO), a proxy for an immune response (Detournay and Weis, 2011). Conversely, LPS challenge of aposymbiotic anemones incubated in Sph led to an increase in the NO signal, indicating initiation of an immune response. Isolated ceramides, the precursors to Sph (Fig. 1), from other cnidarians have also demonstrated both antimicrobial and anti-inflammatory activity when challenged with immune elicitors (Cheng *et al.*, 2009; Al-Lihaibi *et al.*, 2010; Wei *et al.*, 2013). These results suggest a functional role of sphingolipid metabolism in cnidarian pathogenesis and immunity, although the linkage between host sphingolipid-mediated responses in the presence of algal symbionts needs further investigation. Moreover, the involvement of the rheostat during the initial stages of symbiosis from recognition to successful colonization has not been explored.

In this study, we further characterized cnidarian sphingolipids with the quantification of endogenous sphingolipid metabolism in *A. pallida*. This sea anemone is an emerging laboratory model system for the study of cnidarian symbiosis (Weis *et al.*, 2008; Goldstein and King, 2016) because it engages in a symbiosis with *Symbiodinium* spp. and can be maintained in the aposymbiotic state. We predicted that compatible symbionts would drive the host sphingosine rheostat toward cell survival during recolonization and when animals were fully symbiotic. We expanded on the proposed sphingosine rheostat model with quantification of *AP-SPHK* and *AP-SGPP* gene expression, SPHK protein level, and rheostat lipid concentrations in different symbiotic states and newly recolonized anemones. The results suggest that the sphingosine rheostat is shifted toward pro-survival both during onset of symbiosis and in symbiotic anemones.

Materials and Methods

Maintenance of anemone and algal cultures

Symbiotic *Aiptasia pallida* (Agassiz in Verrill, 1864) from Weis Lab population A (VWA; collected from multiple sources in the early 2000s) and the Gisele Muller-Parker population (GMP; collected in Walsingham Pond, Bermuda, in the mid-1980s) were maintained in artificial seawater (ASW) at room temperature (rt; ~25 °C) under 40 μmol quanta m^{-2} s^{-1} on a light/dark cycle of 12 h:12 h. These two populations form associations with the same symbiont, *Symbiodinium minutum* T.C.LaJeunesse, J.E. Parkinson & J.D.Reimer, 2012 (type B1) (Bellis *et al.*, 2016; Grajales *et al.*, 2016), but their host genetics differ based on mitochondrial markers 12S, 16S, and COIII and nuclear marker 28S (Grajales and Rodríguez, 2016). This difference was further confirmed using genome-wide single-nucleotide polymorphisms, where the VWA population is more genetically similar to the clonal line H2 from Hawaii than it is to the GMP population (Bellis *et al.*, 2016). The GMP anemones were used for a pilot experiment of sphingolipid quantification ($n = 3$ anemones for each symbiotic state; data not shown), and a difference in lipid concentrations was observed between the symbiotic and aposymbiotic conditions. Therefore, both populations were examined for gene expression and lipid concentrations, as described below. VWA and GMP aposymbiotic anemones were made by subjecting symbiotic anemones to a series of cold-shock treatments at 4 °C for 6 h twice a week for 6 wk to remove algal symbionts (Muscatine *et al.*, 1991). Aposymbiotic anemones were kept in the dark for at least two months prior to experimentation to prevent symbiont repopulation. Symbiotic and aposymbiotic anemones were fed *Artemia* sp. nauplii twice a week up to at least four days (gene expression) or two weeks (lipid analysis) prior to the commencement of experiments, after which time they were starved. In the recolonization experiment, aposymbiotic VWA anemones were inoculated with *S. minutum* strain CCMP830 (Bigelow Laboratory for Ocean Science, East Boothbay, ME) previously isolated from *A. pallida* (Lesser, 1996). CCMP830 was grown in sterile f/2 media (Guillard and Ryther, 1962) at 25 °C at an irradiance of 40 μmol quanta m^{-2} s^{-1} on a light/dark cycle of 12 h:12 h.

Recolonization experiments

To explore the role of sphingosine rheostat enzymes (AP-SPHK and AP-SGPP) and lipids (S1P and Sph) in the onset of symbiosis, symbiont recolonization of aposymbiotic VWA anemones was examined over three days. Two recolonization experiments were conducted. Animals from the first experiment were prepared for quantitative polymerase chain reac-

tion (qPCR) experiments. A second experiment was conducted for lipid analysis. For the first recolonization experiment, oral and pedal disk diameter (mean 3.93 ± 0.16 mm and 4.08 ± 0.15 mm, respectively) for each anemone was measured with calipers to estimate animal size. In the second recolonization experiment, host size was determined using total host protein, measured with a Bradford assay described below. Material from the first experiment was also used for another unrelated study (Poole *et al.*, 2016), and details of the temporal dynamics of recolonization are described in that study. For both experiments, animals were randomly placed into one of three treatment groups: (1) no symbionts + light (NSL); (2) symbionts + light (SL); and (3) symbionts + dark (SD) (Poole *et al.*, 2016). In the qPCR and lipid experiments, the SL and SD treatment groups were inoculated with 2.19×10^5 ml^{-1} of cultured *S. minutum* and 40 μl of brine shrimp extract, a feeding stimulant used in previous symbiont colonization studies (Schwarz *et al.*, 1999; Weis *et al.*, 2002). The NSL treatment was brought to the same volume as those that received symbionts, with the addition of 1 ml of filtered artificial seawater (FASW) and 40 μl of brine shrimp extract. Treatments NSL and SL were then placed in an incubator at the light and temperature conditions described above. Treatment SD was placed in the dark at rt. After 1 d, anemones were washed with FASW to remove residual symbionts and collected at various time points (0, 0.5, 1, 2, and 3 d after inoculation; qPCR, $n = 3$; lipids, $n = 4$), flash frozen in liquid nitrogen, and stored at −80 °C for processing.

Symbiont quantification

To measure the acquisition of symbionts by *A. pallida* in the recolonization experiments, we quantified algal density using a relative qPCR assay based on the ΔC_t method (Livak and Schmittgen, 2001; Poole *et al.*, 2016). Symbiont quantification from qPCR samples for the symbiotic-state and recolonization experiments was previously analyzed by Poole *et al.* (2016). For recolonized anemones used for lipid analysis, DNA was extracted 3 d after inoculation from 3 additional anemones using a modified cetyltrimethylammonium bromide (CTAB) protocol described by Coffroth *et al.* (1992). Each sample was run in triplicate on a MasterCycler RealPlex^4 machine (Eppendorf, Hamburg, Germany) using 20 ng μl^{-1} of genomic DNA, 0.4 μmol l^{-1} of the gene-specific forward and reverse primers, and SensiFAST SYBR Hi-ROX master mix (Bioline, Boston, MA) according to the manufacturer's protocol. The cycle threshold, or C_t, values were used to calculate relative quantities of 28S rDNA as previously described (Poole *et al.*, 2016).

RNA extraction and cDNA synthesis

Total RNA was extracted from each anemone, using an extraction protocol with TRIzol Reagent (Invitrogen, Carlsbad, CA) and an RNeasy Mini kit (Qiagen, Valencia, CA) described by Poole *et al.* (2016), and stored at −80 °C. RNA quality and quantity were assessed by gel electrophoresis and the NanoDrop ND-1000 (NanoDrop, Wilmington, DE), respectively. Samples with a NanoDrop 260/230 ratio less than 1.5 underwent RNA purification protocol described by Poole *et al.* (2016). Each sample was then treated with the DNA-*free* kit (Ambion, Foster City, CA) or TURBO DNA-*free* kit (Ambion) to remove residual genomic DNA contamination. RNA concentrations were then requantified. cDNA was synthesized using SuperScript III First-Strand Synthesis System (Invitrogen) with 500–750 ng of RNA and 50 μmol l^{-1} of oligo $(dT)_{20}$ primer. Each cDNA sample was diluted to a final concentration of 300 ng μl^{-1} before use in qPCR reactions.

AP-SPHK *and* AP-SGPP *relative qPCR*

The qPCR primers for the genes of interest, *AP-SPHK* and *AP-SGPP*, were previously tested for PCR efficiency and host specificity in a hyperthermal stress study on *A. pallida* (Kitchen and Weis, 2017). These genes were normalized to the reference genes *poly-A binding protein* (*PABP*) and *ribosomal large subunit 10* and *ribosomal large subunit 12* (*L10* and *L12*), selected for their stable expression across symbiotic states and during recolonization (Poole *et al.*, 2016). cDNA from each sample was run in triplicate as 20-μl reactions of 10 μl of *Power* SYBR Green PCR master mix (Applied Biosystems, Foster City, CA), 5 μmol of the forward and reverse primers, 0.5 μl of cDNA, and RNase-free H_2O on the ABI Prism 7500 Real-Time PCR machine (Applied Biosystems) or the StepOnePlus Real-Time PCR machine (Applied Biosystems) with standard settings for 40 cycles. A dissociation curve (95 °C for 15 s, 60 °C for 1 min, ramping temperature gradient [60–95 °C] for 20 min, and 95 °C for 30 s) for the final PCR product was performed to confirm single amplicon detection. No-template, no-reverse transcriptase, and no-primer controls were included as well as at least one interplate calibrator per plate for the symbiotic-state comparison of the GMP anemones and the recolonization experiment. C_t values calculated by ABI 7500 software, version 2.0.6, or StepOne software, version 2.3 (Applied Biosystems), were adjusted for interplate variation and normalized to the geometric mean of the reference genes. Normalized values (ΔC_t) were converted to relative quantities ($\log_2$) by the $\Delta\Delta C_t$ method (Livak and Schmittgen, 2001), with the selected reference samples for each experiment as follows: (1) biological replicate with the lowest expression (highest ΔC_t) from either an aposymbiotic anemone or a symbiotic anemone for each respective gene in the symbiotic-state comparison ($n = 3$ VWA anemones per symbiotic state, $n = 6$ GMP anemones per symbiotic state); (2) mean ΔC_t of treatment group NSL at each time point (0, 0.5, 1, 2, and 3 d; $n = 3$ VWA anemones) for recolonization in the light; and (3) mean ΔC_t of 0-h samples ($n = 6$, combination of aposymbiotic VWA anemones from the symbiotic-state comparison and 0 h experimental controls) for recolonization in

the dark (treatment SD). Relative quantities are presented on the $\log_2$ scale as the mean ± standard error.

Immunoblot of sphingosine kinase

Protein was extracted from aposymbiotic and symbiotic VWA anemones (two anemones per replicate, $n = 3$ replicates) by homogenization in an extraction buffer (100 mmol l^{-1} Tris base, pH 7.4, 100 mmol l^{-1} NaCl, 10 mmol l^{-1} ethylenediaminetetraacetic acid, pH 8.0, with cOmplete Protease Inhibitor Cocktail; Roche, Basel, Switzerland) at a volume of 1 mg ml^{-1} tissue. The supernatant was separated from cellular debris and symbionts through centrifugation at 4 °C for 15 min at 14,000 × *g*. Protein concentrations were determined using a Bradford assay, and 15 μg of sample protein was resuspended in Laemmli buffer (Bio-Rad, Hercules, CA) with 5% 2-mercaptoethanol (Sigma-Aldrich, St. Louis, MO) resolved on 10% Mini-PROTEAN TGX gel (Bio-Rad). Protein was transferred to a 0.45-μm nitrocellulose membrane at 4 °C for 90 min at 75 V using the Mini Trans-Blot unit (Bio-Rad). Protein transfer was verified using Ponceau S stain in 5% acetic acid. The membrane was then blocked overnight at 37 °C with 5% nonfat milk in tris-buffered saline (TBS)-Tween (0.05%) solution, followed by a 15-min wash in TBS-Tween. The membrane was incubated for 1 h at rt with polyclonal anti-SPHK1 (0.375 μg ml^{-1}; Caymen Chemical, Ann Arbor, MI) and washed 5 times for 10 min each in TBS-Tween. The blot was then incubated in secondary goat anti-rabbit IgG horseradish peroxidase (HRP) (0.005 μg ml^{-1}; Caymen Chemical) at rt for 1 h, followed by the same series of washes described above. Bands were detected with Clarity Western enhanced chemiluminescence substrate (Bio-Rad) and exposure to autoradiography film. Relative band intensities were calculated by comparison to the 43-kDa actin band on the Ponceau S-stained blot using ImageJ, version 1.48 (Rasband, 1997–2015). Preliminary tests of anti-SPHK1 using mouse heart homogenate as a positive control showed a single 49-kDa band (data not shown) on immunoblots, as previously reported (Kohama *et al.*, 1998; Olivera *et al.*, 1998).

Lipid extraction and liquid chromatography-tandem mass spectrometry of sphingolipids

Sample lipid extraction followed established protocols (Bligh and Dyer, 1959; Garrett *et al.*, 2013). Two experimental trials were run for the lipid quantification as described by Kitchen and Weis (2017). VWA anemones (for symbiotic and aposymbiotic animals, $n = 8$ in trial 1 and $n = 23$ in trial 2, and for recolonization, $n = 16$ in trial 1) and GMP anemones (for symbiotic and aposymbiotic animals, $n = 21$ in trial 2) were randomly sorted into extraction groups. For each population, the anemones were homogenized in 0.5 ml of 1× phosphate-buffered saline (PBS) and centrifuged at 2500 rpm for 3 min to gently pellet cellular debris and symbionts. The supernatant was divided, with 100 μl set aside for protein quantification using a Bradford assay and the remainder used for lipid extraction. In the first trial, the remaining supernatant was transferred to a 13-mm borosilicate glass tube for lipid extraction using established lipid extraction protocols for *A. pallida* (Garrett *et al.*, 2013; Kitchen and Weis, 2017). In the second trial, lipid extraction from the remaining homogenized tissue was performed by the Lipidomics Core Facility at Wayne State University, Detroit, Michigan. In both trials, an internal standard mixture was added during the extraction, consisting of 25 ng ml^{-1} of C17-base-D-erythro-sphingosine-1-phosphate (C17-S1P) and 25 ng ml^{-1} of C17-base-D-erythro-sphingosine (C17-Sph) (Avanti Polar Lipids, Alabaster, AL).

Target analytes and C17 sphingolipid analogs were resolved by the Lipidomics Core Facility at Wayne State University, as previously described (Kitchen and Weis, 2017). Quality filtered sample S1P and Sph analytes were quantified against internal standards and normalized to total protein, a common proxy for *A. pallida* size (Goulet *et al.*, 2005; Sunagawa *et al.*, 2008). For the recolonization experiment, a fold change was calculated for each sample concentration of treatment group SL referenced to the mean of the concentrations of treatment group NSL at each respective time point.

Statistical analysis

The normality, homoskedasticity, and outlier identification for each respective assay were evaluated using statistical software R, version 3.4.1 (R Core Team, 2017). For symbiont quantification, symbiotic-state qPCR, protein and lipid analyses, and sphingolipid fold changes from recolonized anemones, statistical significance was tested using a nonparametric Mann-Whitney test. Relative quantities ($\log_2$) from the recolonization qPCR assay were analyzed using a multifactor ANOVA with factors including oral disk size (continuous), light (2 levels = light or dark), symbiont (2 levels = symbionts or no symbionts), and time (5 levels = 0, 0.5, 1, 2, and 3 d). The final statistical model for each enzyme was determined through stepwise model tests using the Akaike information criterion. A separate model was fitted with the data for each sphingolipid enzyme mRNA (*AP-SPHK* and *AP-SGPP*), and Tukey's honest significant difference *post hoc* test was performed on ANOVA factors with >2 levels. In all tests, the statistical significant threshold was $P \leq 0.05$.

Results

Sphingosine rheostat expression and metabolism differ with symbiotic state

Using a host-specific qPCR assay (Kitchen and Weis, 2017), gene expression of *AP-SPHK* and *AP-SGPP* was quantified in symbiotic and aposymbiotic anemones for two host populations. Median *AP-SGPP* expression was twofold lower in the symbiotic anemones compared to the aposymbiotic VWA anemones, suggesting a pro-survival cellular response in sym-

biotic *Aiptasia pallida* (Mann-Whitney 1-tailed test, $P = 0.05$; Fig. 2A) and consistent with *SGPP* expression patterns in symbiotic *Anthopleura elegantissima* previously reported (Rodriguez-Lanetty *et al.*, 2006). Although the median *AP-SPHK* expression was slightly upregulated in the symbiotic anemones compared to the aposymbiotic VWA anemones, this difference was not significant (Mann-Whitney 1-tailed test, $P = 0.2$). In the GMP anemones, no difference in median expression of *AP-SPHK* and *AP-SGPP* was observed between the symbiotic and aposymbiotic animals; however, expression of both genes in the symbiotic animals tended to be lower (Mann-Whitney 1-tailed test, *AP-SPHK*, $P = 0.8$; Mann-Whitney test, *AP-SGPP*, $P = 0.24$; Fig. 2B). The individual variation in *AP-SPHK* and *AP-SGPP* expression in the aposymbiotic anemones from both populations was higher than the symbiotic anemones (Fig. 2A, B).

To determine whether differences in mRNA levels would alter cellular protein concentrations, we measured the relative quantity of SPHK protein. In symbiotic VWA anemones, SPHK protein detected in immunoblots was, on average, 49% higher than in aposymbiotic animals; however, the difference was not significant (Mann-Whitney 1-tailed test, $P = 0.1$; Fig. 2G). In preliminary tests of the polyclonal SPHK1 antibody with *A. pallida* protein, we found that it labeled a band with an approximate molecular weight of 75 kDa (Fig. 2G), but the predicted molecular weight of the *AP-SPHK* transcript (National Center for Biotechnology Information: KY038070) is 61 kDa, based on *in silico* estimates. This difference between the estimated and observed molecular weight of AP-SPHK detected with the immunoblots could be a result of post-translational modification, such as phosphorylation, palmitoylation, and acetylation, which has been demonstrated in multiple studies on yeast (Iwaki *et al.*, 2005; Kihara *et al.*, 2005) and vertebrates (reviewed in Chan and Pitson, 2013).

To assess the functioning of the rheostat and to determine whether it changes with symbiotic state, we quantified S1P and Sph concentrations in two populations of *A. pallida*. The cellular concentrations of S1P and Sph in *A. pallida* were consistent with studies in other organisms, where S1P can be 1/100th the concentration of Sph under stable conditions (Maceyka *et al.*, 2005; Shaner *et al.*, 2009). Based on the trend of higher relative expression of *AP-SPHK* compared to *AP-SGPP* in symbiotic anemones in both populations and slightly higher protein abundance in symbiotic VWA anemones, we predicted elevated cellular S1P concentrations in symbiotic anemones. There was no difference in S1P concentrations between symbiotic states in the VWA population (Fig. 2C). However, this pattern was observed in the GMP population (Fig. 2D). The median S1P concentration was significantly higher by 0.84 ng mg^{-1} protein in symbiotic compared to aposymbiotic anemones (Mann-Whitney 1-tailed test, $P < 0.001$). In contrast, the median Sph concentration differed between symbiotic states of the VWA anemones (Mann-Whitney 1-tailed test, $P = 0.018$; Fig. 2E), which is consistent with the observed gene expression differences of *AP-SGPP* (Fig. 2A). There was no difference in Sph concentrations in the GMP population (Fig. 2F).

In addition to their role in mediating microbe interactions, the rheostat enzymes maintain an intracellular balance of the bioactive sphingolipids during homeostasis. At rest the cellular S1P levels are low (Schwab, 2005), but an upregulation of SPHK enzymatic activity and S1P initiates the recycling action of SGPP (Fig. 1). The relationship of the gene expression between the rheostat enzymes was compared by symbiotic state. When both populations were combined, a significant positive correlation between the expression of the rheostat genes was observed in the symbiotic anemones (Pearson's product-moment correlation, $R^2 = 0.79$, $P = 0.012$; Fig. 3A). Similarly, a significant positive correlation was found between cellular S1P and Sph concentrations in symbiotic anemones (Pearson's product-moment correlation, $R^2 = 0.78$, $P < 0.001$; Fig. 3B).

Host rheostat gene expression, but not necessarily sphingolipids, is altered during host recolonization by symbionts

We predicted that the rheostat would shift toward pro-survival during onset of the beneficial cnidarian-*Symbiodinium* symbiosis. To assess changes in gene expression during onset of symbiosis, we used a set of VWA anemones that were also used in a study investigating the complement system, which is part of the innate immune response in cnidarians (Poole *et al.*, 2016).

To understand the dynamics of host recolonization by symbionts across our time course in both gene expression and lipid analyses, we measured relative symbiont abundance using a qPCR assay of *Symbiodinium minutum* 28S rDNA described by Poole *et al.* (2016). After 1 d after inoculation, the relative abundance of symbionts from the recolonized anemones used for qPCR significantly increased in both SL and SD treatment groups compared to aposymbiotic anemones, indicating the successful uptake of symbionts (Poole *et al.*, 2016). Furthermore, the relative symbiont abundance of anemones in the SL group continued to increase between days 1 and 3, whereas the SD group decreased slightly (Poole *et al.*, 2016). In the anemones used for lipid analysis, the mean relative $\log_2$ quantities of symbiont 28S rDNA at 3 d after inoculation for the SL group was 7.92 ± 0.26, which was 22% lower than those reported for the previous recolonized samples used to measure gene expression (Mann-Whitney 1-tailed test, $P = 0.05$). Nevertheless, because anemones were washed 1 d after inoculation, increased symbiont densities at 3 d in the SL treatment from both recolonization experiments could be a result of symbiont proliferation within the host tissue, which suggests successful establishment of symbiosis.

The expression of *AP-SPHK* and *AP-SGPP* displayed significant interactions of time and recolonization and of time and light treatments in the respective comparison groups

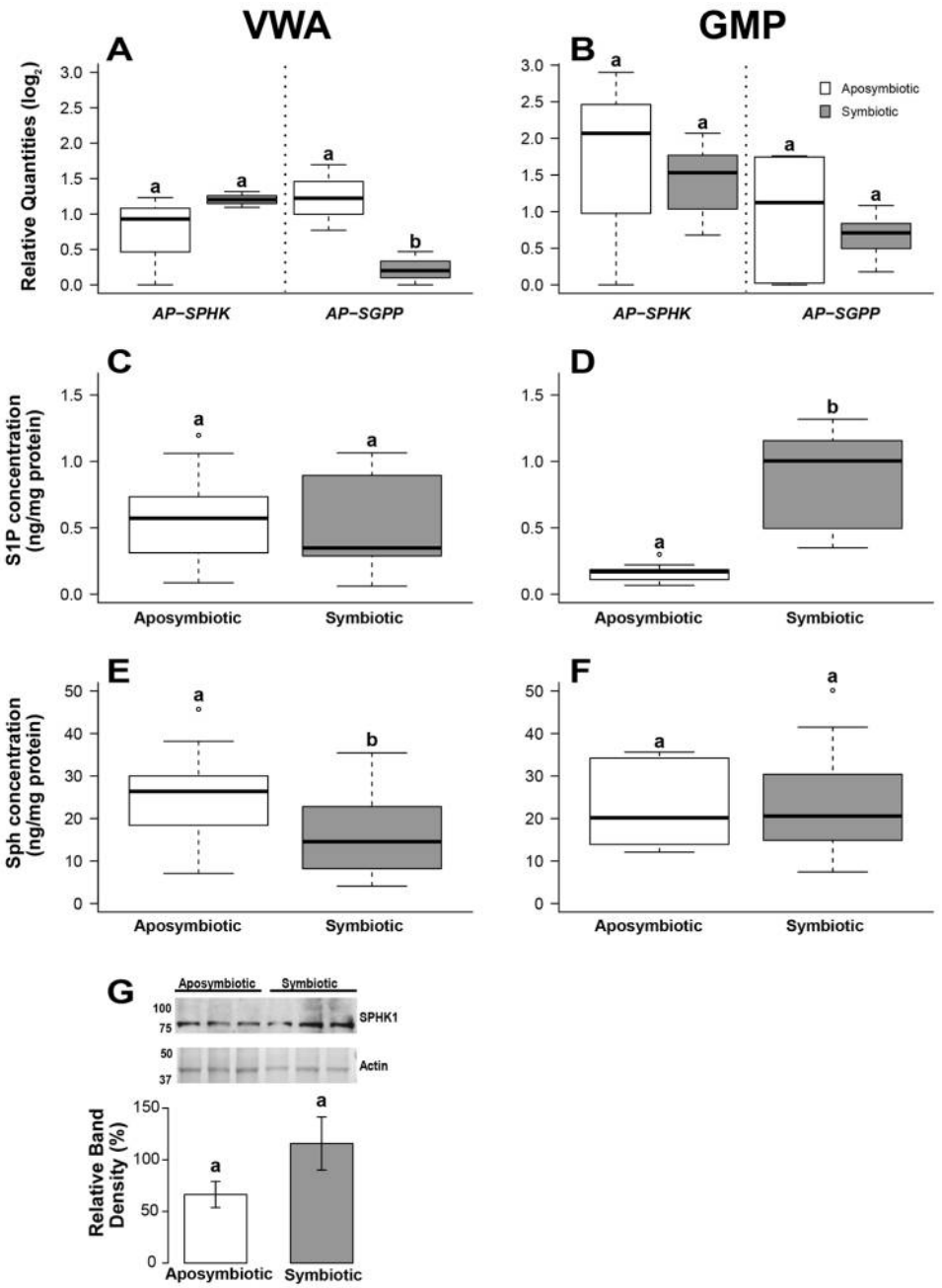

Figure 2. Rheostat gene expression, immunodetection, and lipid concentration of *Aiptasia pallida* from two host populations in different symbiotic states. RNA and protein and lipid extracts were extracted from symbiotic (gray) or aposymbiotic (white) anemones in steady state from Weis Lab population A (VWA) and the Gisele Muller-Parker population (GMP). cDNA from (A) VWA and (B) GMP sample RNA was used to quantify relative mRNA quantities ($\log_2$) of *AP-SPHK* and *AP-SGPP* with quantitative polymerase chain reaction ($n = 3$ VWA anemones per group, $n = 6$ GMP anemones per group). Lipid concentrations (ng mg^{-1} protein) of (C, D) sphingosine-1-phosphate (S1P) and (E, F) sphingosine (Sph) were quantified from (C, E) VWA and (D, F) GMP anemone lipid extracts (VWA: $n = 16$ aposymbiotic anemones and $n = 15$ symbiotic anemones; GMP: $n = 10$ aposymbiotic anemones and $n = 11$ symbiotic anemones) after high-performance liquid chromatography resolution electrospray ionization-tandem mass spectrometry, then normalized to internal standards (ng ml^{-1}) and host protein (mg ml^{-1}). Immunoblots of VWA anemones in different states ($n = 3$ per symbiotic state) were probed with rabbit polyclonal antibody against human SPHK1 (sphingosine kinase 1) (G, upper panel). The band intensity of SPHK (75 kDa) was calculated relative to the actin band, 43 kDa, in the Ponceau S (Pon-S)-stained blot ($n = 2$ blots; G, lower panel). Values represent the mean ± standard error. (A–F) Boxplots display the distribution of the data, where the solid line in the box is the median, the box is the upper and lower quartiles, and bracketed lines are maximum and minimum values. Differences in lowercase letters indicate significant differences ($P \leq 0.05$) between symbiotic states for each respective analysis determined with 1-tailed Mann-Whitney tests.

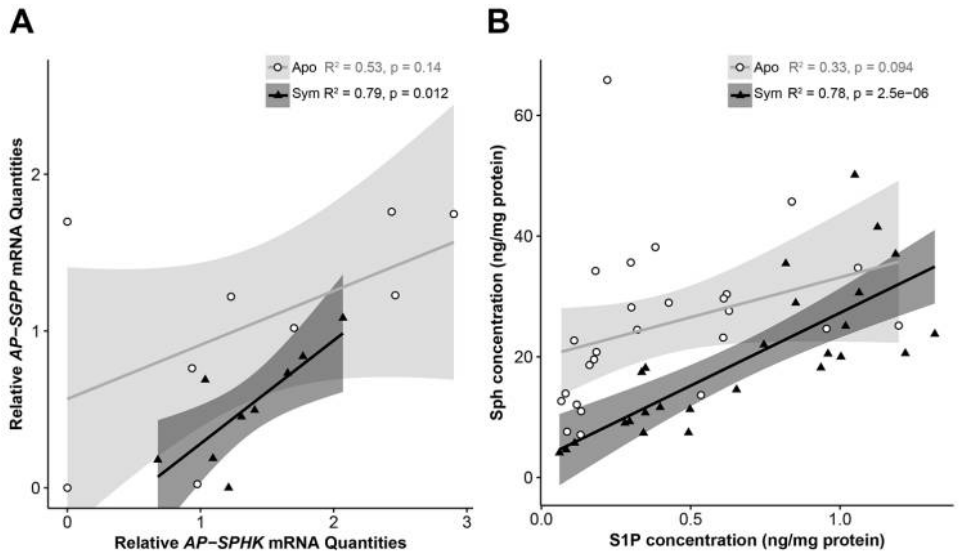

Figure 3. Positive correlation between *AP-SPHK* and *AP-SGPP* expression and sphingolipid concentrations in symbiotic *Aiptasia pallida*. Correlations between the relative mRNA quantities of (A) the rheostat genes and (B) the sphingolipids from both Weis Lab population A (VWA) and the Gisele Muller-Parker population (GMP) of symbiotic and aposymbiotic anemones were compared using a Pearson's product-moment correlation test. A significant positive correlation was found between the expression of the 2 genes ($n = 9$ per symbiotic state; $P = 0.012$) and the 2 lipids in symbiotic anemones ($n = 26$ per symbiotic state; $P < 0.001$). The best-fit line is shown for each respective group, and the shaded area depicts the 95% confidence intervals.

(Table 1) but did not differ with anemone size (ANOVA, $P > 0.05$). *AP-SPHK* mean expression increased by 2.09- and 6.22-fold in the SL treatment group at 0.5 h and 1 d, respectively (Tukey *post hoc*, $P < 0.001$; Fig. 4A) before returning to levels not significantly different from the NSL control group by 2 d after inoculation. Therefore, initial elevations of *AP-SPHK* corresponded with the symbiont uptake (Poole *et al.*, 2016). *AP-SGPP* expression also increased in the SL anemones at 0.5 and 1 d but only by 1.16 and 2.15 times that of the NSL group (Tukey *post hoc*, $P = 0.007$; Fig. 4B). At day 3 in the SL treatment group, *AP-SPHK* expression did not change, but *AP-SGPP* was significantly upregulated by 1.97-fold (Tukey *post hoc*, $P < 0.001$; Fig. 4B). In addition to measuring symbiont recolonization and rheostat modulation in the light, we investigated how incubation in the dark influenced recolonization. Given that the translocation of photosynthetic products from symbiont to host is central to the cnidarian-*Symbiodinium* symbiosis, uptake of symbionts in the dark would be less favorable for symbiosis establishment. The downregulation of *AP-SPHK* and *AP-SGPP* in the SD treatment significantly dif-

Table 1

ANOVA results for gene expression of AP-SPHK *and* AP-SGPP *during the recolonization experiment*

Gene	Comparisons	Factors	SS	df	*F*	*P*-value
AP-SPHK	SL *vs.* NSL	Time	54.25	4	41.57	<0.001
		Symbiont	23.27	1	71.33	<0.001
		Time : symbiont	34.32	3	16.43	<0.001
	SL *vs.* SD	Time	136.76	4	59.26	<0.001
		Light	27.68	1	47.97	<0.001
		Time : light	7.00	3	3.76	0.029
AP-SGPP	SL *vs.* NSL	Time	6.96	4	14.38	<0.001
		Symbiont	10.12	1	83.60	<0.001
		Time : symbiont	3.688	3	7.438	0.001
	SL *vs.* SD	Time	21.28	4	30.05	<0.001
		Light	3.89	1	21.98	<0.001
		Time : light	9.46	3	17.81	<0.001

Factors were selected based on the Akaike information criterion for statistical model testing. Sum of squares (SS), degrees of freedom (df), *F*-statistics, and *P*-values were rounded to the nearest hundredth. NSL, no symbionts + light; SD, symbionts + dark; SL, symbionts + light.

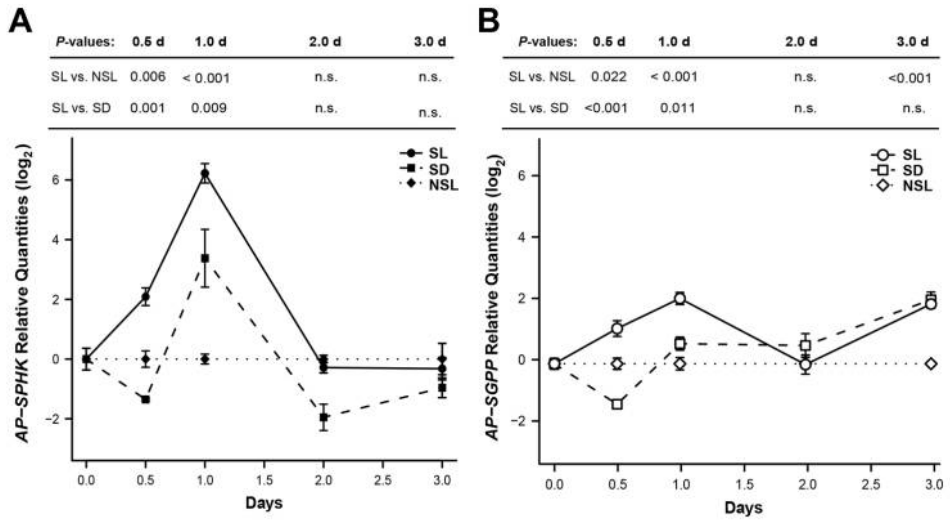

Figure 4. Symbiont uptake by hosts in the light and the dark modulates *AP-SPHK* and *AP-SGPP* expression. Aposymbiotic *Aiptasia pallida* were inoculated with 10^5 *Symbiodinium minutum* strain CCMP830 (type B1) and washed 1 d after inoculation. Relative mRNA quantities ($\log_2$) of (A) *AP-SPHK* and (B) *AP-SGPP* were quantified over time using quantitative polymerase chain reaction in recolonized anemone cDNA from light only (NSL, diamonds), symbiont + light (SL, circles), and symbiont + dark (SD, square) treatment groups. Relative quantities are presented as the mean ± standard error ($n = 3$ anemones for each time point within each treatment group). Results of the Tukey *post hoc* comparisons from the ANOVA are presented above (A) and (B). Comparisons that were not significant (n.s.) did not pass the $P \leq 0.05$ threshold.

fered at 0.5 d after inoculation from the SL treatment group (Tukey *post hoc*, $P < 0.001$; Fig. 4). Expression of both genes was then upregulated at 1 d but significantly less than in the SL group (Fig. 4).

To examine whether changes in sphingosine rheostat expression corresponded to concomitant changes in sphingolipid levels during recolonization, we quantified S1P and Sph concentrations in SL and NSL treatment groups at 1 and 3 d of recolonization and calculated a ratio of SL : NSL. A fold change of 1 indicates no difference in the recolonized anemone lipid levels compared to those in time-matched NSL anemones. The low concentration of S1P in our samples made detection difficult and 2 samples, one in the NSL group at 3 d and one in the SL group at 1 d, were detected as outliers and removed from the analysis. From the remaining samples, there were trends in lipid level changes with time but no significant differences. At 1 d, the median S1P fold change was lower than 1, with SL anemone lipid concentrations below those of the control NSL group, whereas the median Sph fold change was higher than 1 (Fig. 5). At 3 d, trends in lipid levels were opposite those at 1 d, where median S1P and Sph fold changes were higher and lower in the SL treatment, respectively (Fig. 5).

Discussion

A regulatory role for the host sphingosine rheostat in maintaining cnidarian-*Symbiodinium* symbiosis has been hypothesized previously, based on functional genomic evidence (Rodriguez-Lanetty *et al.*, 2006). We tested this hypothesis empirically through quantification of *AP-SPHK* and *AP-SGPP* gene expression, SPHK protein abundance, and S1P and Sph sphingolipid concentrations in different symbiotic states and newly recolonized *Aiptasia pallida*.

Comparison of gene expression, protein abundance, and lipid concentrations between the symbiotic and aposymbiotic states suggests that the presence of algal symbionts in *A. pallida* shifts the rheostat toward a pro-survival state. Reduced Sph concentrations corresponded with reduced *AP-SGPP* gene expression in symbiotic VWA anemones, suggesting protection against apoptosis when symbionts are present. We also observed modest changes in *AP-SPHK* expression in VWA and GMP anemones and in protein quantities in VWA anemones that could be sufficient to generate differences in cellular S1P levels between symbiotic states. Increased cellular S1P was observed in the symbiotic GMP anemones despite detecting no significant differences in *AP-SPHK* expression between symbiotic states. In other animal systems, slight enhancement of *SPHK* expression and activity by just 1.5- to 2-fold resulted in rapid S1P production (Pitson *et al.*, 2000, 2003). These snapshots of rheostat function based on symbiotic state suggest that the host rheostat is a dynamic physiological mechanism that plays a role in the regulation of symbiosis.

To maintain homeostasis, the coordinated activities of both enzymes are important to monitor and maintain the cellular levels of signaling sphingolipids (Fig. 1). The correlation between the relative mRNA quantities of *AP-SPHK* and *AP-SGPP* and their corresponding lipid metabolites in symbiotic anem-

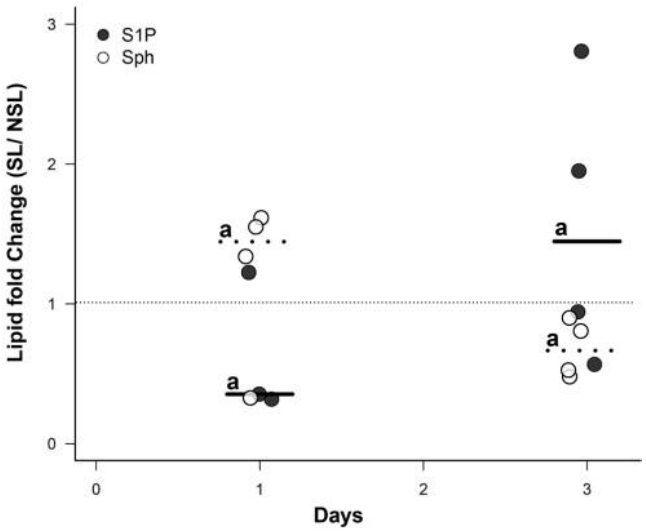

Figure 5. Fold change of host sphingolipids during symbiont recolonization. Lipid extracts ($n = 4$ per time point, except sphingosine-1-phosphate [S1P] at 1 d, where $n = 3$) were quantified with high-performance liquid chromatography resolution electrospray ionization-tandem mass spectrometry, normalized to internal standards and total protein. Calculated fold changes of S1P (filled circles) and sphingosine (Sph, open circles) for treatment groups SL (symbiont + light) and NSL (no symbionts + light) at 1 and 3 d were analyzed with 1-tailed Mann-Whitney tests. Solid (S1P) and dashed (Sph) bars show the median fold change for each metabolite at the separate days. The letter above the solid or dashed lines indicates the significance of a 1-tailed Mann-Whitney test (S1P, $P = 0.114$; Sph, $P = 0.171$). Groups sharing a letter (a) do not significantly differ ($P \leq 0.05$).

ones supports the hypothesis that these enzymes play a role in homeostatic balance.

A population difference emerged in the study, where the two sphingolipid levels varied between the symbiotic anemones of the same species. While a similar trend toward a pro-survival shift in the rheostat was present in both symbiotic groups from the two populations, there were differences in rheostat gene expression and lipid concentrations by population. This difference in sphingolipid metabolism at the population level suggests that pairing of the host and/or symbiont genetic background could modify host rheostat function. Further investigation of host expression, protein abundance, and lipid levels captured simultaneously from other *A. pallida* populations is needed to understand the influence of host genetics or partner pairings on rheostat-mediated symbiosis regulation.

Our study also provides evidence that the sphingosine rheostat expression is modified during recolonization of *A. pallida* by *Symbiodinium minutum*. During recolonization in the light, symbionts were observed within hosts as early as 1 d after inoculation, which corresponded with changes in *AP-SPHK* and *AP-SGPP* expression. The upregulation of *AP-SPHK* was approximately 4 times higher than *AP-SGPP* at 1 d after inoculation, indicating an overall shift in the rheostat toward host cell survival with the uptake of *S. minutum*. As seen with the fully symbiotic anemones, elevated *AP-SPHK* is correlated with elevated *AP-SGPP* in recolonizing *A. pallida*. Therefore, the upregulation of *AP-SGPP* could help with the metabolic turnover of the sphingolipids after symbiont uptake. The pro-survival shift in the recolonized symbiotic anemones is similar to that observed by lung epithelial cells infected with respiratory syncytical virus. This virus increases cellular S1P by combined activation of ceramidase, an enzyme that degrades pro-apoptotic ceramide to Sph (Fig. 1), and SPHK, thereby delaying host cell death and facilitating viral replication (Monick *et al.,* 2004).

Symbiont recolonization in the dark also altered the sphingosine rheostat expression with an upregulation of both genes at 1 d after inoculation, albeit significantly less so than recolonization in the light. Prolonged incubation in darkness repressed both host recolonization success and rheostat gene expression, suggesting that light and possibly photosynthetic performance by the algae are key for symbiont population growth and ultimately for the symbiosis to reach a stable state. Previous studies of symbiosis-linked host genes such as *sym32* (Ganot *et al.*, 2011) and complement genes Factor B and mannose-binding lectin-associated serine protease (Poole *et al.*, 2016) have identified light-induced expression patterns. In this study, upregulation of rheostat genes at day 1 in the light and dark during recolonization suggests that rheostat-mediated regulation is not dependent on light but is related to the presence of symbionts. Unlike recolonization at day 1, the upregulation of *AP-SGPP* at 3 d after inoculation in both the light and the dark does not have a clear pattern associated with the symbiont recolonization dynamics observed in this study. We hypothesize that the additional *AP-SGPP* mRNA in both light conditions could result from a need to bring the cell toward homeostatic lipid concentrations after symbiont uptake or could be associated with other cellular events triggered after phagocytosis of *S. minutum*, such as post-winnowing mechanisms. Additional studies are required to determine how these fluxes in rheostat gene expression and their downstream effectors function in symbiosis onset in *A. pallida*.

From the lipid analysis, we aimed to link the temporal patterns of rheostat gene expression to changes in sphingolipids levels, an indirect measure of enzyme activity. Unfortunately, no significant differences in lipid concentrations were detected. Nonetheless, there was a trend in the lipid levels over time, with higher median S1P fold change occurring at 3 d after inoculation following upregulation of the rheostat enzymes at 1 d after inoculation. The upregulation of *AP-SGPP* but not *AP-SPHK* at 3 d after inoculation suggests an increase in cellular Sph levels with a decrease in S1P, but this was not observed in the SL-treated anemones. This lack of difference in lipid concentrations could be the result of multiple factors, for example: (1) the lower symbiont abundance in the second recolonization experiment could have delayed rheostat expression and activity, (2) the number of gastrodermal cells interacting with symbionts could have been too low to detect a difference in sphingolipids when measured from the whole organism,

or (3) the timescale (over days) used to capture transient sphingolipid signaling could have been too long. Other host-microbe studies have detected measurable differences in sphingolipids over hours of colonization (Xia *et al.*, 2002; Prakash *et al.*, 2010). While the underlying mechanisms for the delay in S1P or Sph production need to be addressed in future studies, the modest increase of S1P levels may trigger pro-survival pathways including MAP kinase and Akt that, when inhibited in *A. pallida*, result in increased symbiont loss (Dunn *et al.*, 2007). Direct measurement of SPHK and SGPP enzymatic activity during recolonization and from different symbiotic states in the future will help resolve the timing of S1P production and its importance in symbiont recognition.

The rheostat-mediated response during host-microbe interactions is dependent on the mode of entry, duration of the interaction, and type of partner. In the case of *A. pallida*, we provide some evidence for symbiosis regulation by the cnidarian sphingosine rheostat with a shift in favor of cell survival through changes in the rheostat in the presence of *S. minutum* during the establishment and maintenance of symbiosis. This pattern is also observed during recolonization of hosts by symbionts, suggesting a role for the host rheostat in managing *S. minutum* colonization during initial contact and phagocytosis. This is the first step in studying the role of the sphingosine rheostat in regulating the onset and colonization of symbionts in a cnidarian host. Sphingolipid metabolism has been linked to macrophage phagocytosis of other microbes (Thompson *et al.*, 2005; Tafesse *et al.*, 2015), pointing to a potentially conserved mechanism for microbe recognition and sorting in metazoans.

Acknowledgments

This work was funded by grants IOB0919073 and IOB1529059 from the National Science Foundation awarded to VMW and grants from the Department of Integrative Biology at Oregon State University awarded to SAK. The authors would like to thank Trevor Tivey, Kinsey Matthews, and Darian Thompson for their assistance in the execution of the study. We would also like to thank Dr. Robert Mason for technical advice and help with the lipid extractions and Drs. Iliana Baums and James Marden for use of their laboratory space and equipment at Pennsylvania State University. In addition, we would like to thank Drs. Dee Denver, John Fowler, Nathan Kirk, Eli Meyer, and Barbara Taylor and the reviewers for their valuable comments on the manuscript.

Literature Cited

Al-Lihaibi, S. S., S.-E. N. Ayyad, F. Shaher, and W. M. Alarif. 2010. Antibacterial sphingolipid and steroids from the black coral *Antipathes dichotoma*. *Chem. Pharm. Bull. (Tokyo)* **58:** 1635–1638.

Ali, H. Z., C. R. Harding, and P. W. Denny. 2011. Endocytosis and sphingolipid scavenging in *Leishmania mexicana* amastigotes. *Biochem. Res. Intl.* **2012:** 691363.

An, D., S. F. Oh, T. Olszak, J. F. Neves, F. Y. Avci, D. Erturk-Hasdemir, X. Lu, S. Zeissig, R. S. Blumberg, and D. L. Kasper. 2014. Sphingolipids from a symbiotic microbe regulate homeostasis of host intestinal natural killer T cells. *Cell* **156:** 123–133.

An, S., T. Bleu, W. Huang, O. G. Hallmark, S. R. Coughlin, and E. J. Goetzl. 1997. Identification of cDNAs encoding two G protein-coupled receptors for lysosphingolipids. *FEBS Lett.* **417:** 279–282.

Bellis, E. S., D. K. Howe, and D. R. Denver. 2016. Genome-wide polymorphism and signatures of selection in the symbiotic sea anemone *Aiptasia*. *BMC Genomics* **17:** 160.

Bligh, E. G., and W. J. Dyer. 1959. A rapid method of total lipid extraction and purification. *Can. J. Biochem. Physiol.* **37:** 911–917.

Chan, H., and S. M. Pitson. 2013. Post-translational regulation of sphingosine kinases. *Biochim. Biophys. Acta* **1831:** 147–156.

Chen, H.-K., S.-N. Song, L.-H. Wang, A. B. Mayfield, Y.-J. Chen, W.-N. U. Chen, and C.-S. Chen. 2015. A compartmental comparison of major lipid species in a coral-*Symbiodinium* endosymbiosis: evidence that the coral host regulates lipogenesis of its cytosolic lipid bodies. *PLoS One* **10:** e0132519.

Cheng, S., Z. Wen, S. Chiou, C. Tsai, S. Wang, C. Hsu, C. Dai, M. Chiang, W. Wang, and C. Duh. 2009. Ceramide and cerebrosides from the octocoral *Sarcophyton ehrenbergi*. *J. Nat. Prod.* **72:** 465–468.

Cinque, B., L. Di Marzio, C. Centi, C. Di Rocco, C. Riccardi, and M. G. Cifone. 2003. Sphingolipids and the immune system. *Pharmacol. Res.* **47:** 421–437.

Coffroth, M. A., H. R. Lasker, M. E. Diamond, J. A. Bruenn, and E. Bermingham. 1992. DNA fingerprints of a gorgonian coral: a method for detecting clonal structure in a vegetative species. *Mar. Biol.* **114:** 317–325.

Cuvillier, O., G. Pirianov, B. Kleuser, P. G. Vanek, O. A. Coso, J. S. Gutkind, and S. Spiegel. 1996. Suppression of ceramide-mediated programmed cell death by sphingosine-1-phosphate. *Nature* **381:** 800–803.

Davy, S. K., D. Allemand, and V. M. Weis. 2012. Cell biology of cnidarian-dinoflagellate symbiosis. *Microbiol. Mol. Biol. Rev.* **76:** 229–261.

Detournay, O., and V. M. Weis. 2011. Role of the sphingosine rheostat in the regulation of cnidarian-dinoflagellate symbioses. *Biol. Bull.* **221:** 261–269.

Dunn, S. R., C. E. Schnitzler, and V. M. Weis. 2007. Apoptosis and autophagy as mechanisms of dinoflagellate symbiont release during cnidarian bleaching: Every which way you lose. *Proc. R. Soc. Biol. Sci. B* **274:** 3079–3085.

Dunn, S. R., M. C. Thomas, G. W. Nette, and S. G. Dove. 2012. A lipidomic approach to understanding free fatty acid lipogenesis derived from dissolved inorganic carbon within cnidarian-dinoflagellate symbiosis. *PLoS One* **7:** e46801.

Ganot, P., A. Moya, V. Magnone, D. Allemand, P. Furla, and C. Sabourault. 2011. Adaptations to endosymbiosis in a cnidarian-dinoflagellate association: differential gene expression and specific gene duplications. *PLoS Genet.* **7:** e1002187.

Garrett, T. A., J. L. Schmeitzel, J. A. Klein, J. J. Hwang, and J. A. Schwarz. 2013. Comparative lipid profiling of the cnidarian *Aiptasia pallida* and its dinoflagellate symbiont. *PLoS One* **8:** e57975.

Goldstein, B., and N. King. 2016. The future of cell biology: emerging model organisms. *Trends Cell Biol.* **26:** 818–824.

Goulet, T. L., C. B. Cook, and D. Goulet. 2005. Effect of short-term exposure to elevated temperatures and light levels on photosynthesis of different host-symbiont combinations in the *Aiptasia pallida*/*Symbiodinium* symbiosis. *Limnol. Oceanogr.* **50:** 1490–1498.

Grajales, A., and E. Rodriguez. 2014. Morphological revision of the genus *Aiptasia* and the family Aiptasiidae (Cnidaria, Actiniaria, Metridioidea). *Zootaxa* **3826:** 55–100.

Grajales, A., and E. Rodríguez. 2016. Elucidating the evolutionary relationships of the Aiptasiidae, a widespread cnidarian-dinoflagellate model system (Cnidaria: Anthozoa: Actiniaria: Metridioidea). *Mol. Phylogenet. Evol.* **94:** 252–263.

Grajales, A., E. Rodríguez, and D. J. Thornhill. 2016. Patterns of *Symbiodinium* spp. associations within the family Aiptasiidae, a monophyletic lineage of symbiotic of sea anemones (Cnidaria, Actiniaria). *Coral Reefs* **35:** 345–355.

Guillard, R. R. L., and J. H. Ryther. 1962. Studies of marine planktonic diatoms. I. *Cyclotella nana* Hustedt and *Detonula confervacea* Cleve. *Can. J. Microbiol.* **8:** 229–239.

Heung, L. J., C. Luberto, and M. Del Poeta. 2006. Role of sphingolipids in microbial pathogenesis. *Infect. Immun.* **74:** 28–39.

Imbs, A. B., I. M. Yakovleva, and L. Q. Pham. 2010. Distribution of lipids and fatty acids in the zooxanthellae and host of the soft coral *Sinularia* sp. *Fish. Sci.* **76:** 375–380.

Iwaki, S., A. Kihara, T. Sano, and Y. Igarashi. 2005. Phosphorylation by Pho85 cyclin-dependent kinase acts as a signal for the down-regulation of the yeast sphingoid long-chain base kinase Lcb4 during the stationary phase. *J. Biol. Chem.* **280:** 6520–6527.

Kellogg, R. B., and J. S. Patton. 1983. Lipid droplets, medium of energy exchange in the symbiotic anemone *Condylactis gigantea*: a model coral polyp. *Mar. Biol.* **75:** 137–149.

Kihara, A., F. Kurotsu, T. Sano, S. Iwaki, and Y. Igarashi. 2005. Long-chain base kinase Lcb4 is anchored to the membrane through its palmitoylation by Akr1. *Mol. Cell. Biol.* **25:** 9189–9197.

Kitchen, S. A., and V. M. Weis. 2017. The sphingosine rheostat is involved in the cnidarian heat stress response but not necessarily in bleaching. *J. Exp. Biol.* **220:** 1709–1720.

Kohama, T., A. Olivera, L. Edsall, M. M. Nagiec, R. Dickson, and S. Spiegel. 1998. Molecular cloning and functional characterization of murine sphingosine kinase. *J. Biol. Chem.* **273:** 23722–23728.

Lesser, M. P. 1996. Elevated temperatures and ultraviolet radiation cause oxidative stress and inhibit photosynthesis in symbiotic dinoflagellates. *Limnol. Oceanogr.* **41:** 271–283.

Livak, K. J., and T. D. Schmittgen. 2001. Analysis of relative gene expression data using real-time quantitative PCR and the $2^{-\Delta\Delta C_T}$ method. *Methods* **25:** 402–408.

Maceyka, M., S. G. Payne, S. Milstien, and S. Spiegel. 2002. Sphingosine kinase, sphingosine-1-phosphate, and apoptosis. *Biochim. Biophys. Acta* **1585:** 193–201.

Maceyka, M., H. Sankala, N. C. Hait, H. Le Stunff, H. Liu, R. Toman, C. Collier, M. Zhang, L. S. Satin, A. H. Merrill, *et al*. 2005. SphK1 and SphK2, sphingosine kinase isoenzymes with opposing functions in sphingolipid metabolism. *J. Biol. Chem.* **280:** 37118–37129.

Mandala, S. M., R. Thornton, Z. Tu, M. B. Kurtz, J. Nickels, J. Broach, R. Menzeleev, and S. Spiegel. 1998. Sphingoid base 1-phosphate phosphatase: a key regulator of sphingolipid metabolism and stress response. *Proc. Natl. Acad. Sci. U.S.A.* **95:** 150–155.

Monick, M. M., K. Cameron, L. S. Powers, N. S. Butler, D. McCoy, R. K. Mallampalli, and G. W. Hunninghake. 2004. Sphingosine kinase mediates activation of extracellular signal-related kinase and Akt by respiratory syncytial virus. *Am. J. Respir. Cell Mol. Biol.* **30:** 844–852.

Muscatine, L., D. Grossman, and J. Doino. 1991. Release of symbiotic algae by tropical sea anemones and corals after cold shock. *Mar. Ecol. Prog. Ser.* **77:** 233–243.

Olivera, A., and S. Spiegel. 2001. Sphingosine kinase: a mediator of vital cellular functions. *Prostaglandins Other Lipid Mediat.* **64:** 123–134.

Olivera, A., T. Kohama, Z. Tu, S. Milstien, and S. Spiegel. 1998. Purification and characterization of rat kidney sphingosine kinase. *J. Biol. Chem.* **273:** 12576–12583.

Olivera, A., H. M. Rosenfeldt, M. Bektas, F. Wang, I. Ishii, J. Chun, S. Milstien, and S. Spiegel. 2003. Sphingosine kinase type 1 induces G12/13-mediated stress fiber formation, yet promotes growth and survival independent of G protein-coupled receptors. *J. Biol. Chem.* **278:** 46452–46460.

Peng, S.-E., W.-N. U. Chen, H.-K. Chen, C.-Y. Lu, A. B. Mayfield, L.-S. Fang, and C.-S. Chen. 2011. Lipid bodies in coral-dinoflagellate endosymbiosis: proteomic and ultrastructural studies. *Proteomics* **11:** 3540–3555.

Pitson, S. M., P. A. Moretti, J. R. Zebol, P. Xia, J. R. Gamble, M. A. Vadas, R. J. D'Andrea, and B. W. Wattenberg. 2000. Expression of a catalytically inactive sphingosine kinase mutant blocks agonist-induced sphingosine kinase activation A dominant-negative sphingosine kinase. *J. Biol. Chem.* **275:** 33945–33950.

Pitson, S. M., P. A. Moretti, J. R. Zebol, H. E. Lynn, P. Xia, M. A. Vadas, and B. W. Wattenberg. 2003. Activation of sphingosine kinase 1 by ERK1/2-mediated phosphorylation. *EMBO J.* **22:** 5491–5500.

Poole, A. Z., S. A. Kitchen, and V. M. Weis. 2016. The role of complement in cnidarian-dinoflagellate symbiosis and immune challenge in the sea anemone *Aiptasia pallida*. *Front. Microbiol.* **7:** 519.

Prakash, H., A. Luth, N. Grinkina, D. Holzer, R. Wadgaonkar, A. P. Gonzalez, E. Anes, and B. Kleuser. 2010. Sphingosine kinase-1 (SphK-1) regulates *Mycobacterium smegmatis* infection in macrophages. *PLoS One* **5:** e10657.

R Core Team. 2017. R: a language and environment for statistical computing. [Online]. R Foundation for Statistical Computing, Vienna. Available: https://www.R-project.org [2017, October 18].

Rasband, W. 1997–2015. ImageJ. [Online]. U.S. National Institutes of Health, Bethesda, MD. Available: http://imagej.nih.gov/ij/ [2017, December 8].

Revel, J., L. Massi, M. Mehiri, M. Boutoute, P. Mayzaud, L. Capron, and C. Sabourault. 2016. Differential distribution of lipids in epidermis, gastrodermis and hosted *Symbiodinium* in the sea anemone *Anemonia viridis*. *Comp. Biochem. Physiol. A Mol. Integr. Physiol.* **191:** 140–151.

Rivera, J., R. L. Proia, and A. Olivera. 2008. The alliance of sphingosine-1-phosphate and its receptors in immunity. *Nat. Rev. Immunol.* **8:** 753–763.

Rodriguez-Lanetty, M., W. Phillips, and V. Weis. 2006. Transcriptome analysis of a cnidarian-dinoflagellate mutualism reveals complex modulation of host gene expression. *BMC Genomics* **7:** 23.

Schwab, S. R., J. P. Pereira, M. Matloubian, Y. Xu, Y. Huang, and J. G. Cyster. 2005. Lymphocyte sequestration through S1P lyase inhibition and disruption of S1P gradients. *Science* **309:** 1735–1739.

Schwarz, J. A., D. A. Krupp, and V. M. Weis. 1999. Late larval development and onset of symbiosis in the scleractinian coral *Fungia scutaria*. *Biol. Bull.* **196:** 70–79.

Shaner, R. L., J. C. Allegood, H. Park, E. Wang, S. Kelly, C. A. Haynes, M. C. Sullards, and A. H. Merrill. 2009. Quantitative analysis of sphingolipids for lipidomics using triple quadrupole and quadrupole linear ion trap mass spectrometers. *J. Lipid Res.* **50:** 1692–1707.

Simon, G., and G. Rouser. 1967. Phospholipids of the sea anemone: quantitative distribution; absence of carbon-phosphorus linkages in glycerol phospholipids: structural elucidation of ceramide aminoethylphosphonate. *Lipids* **2:** 55–59.

Spiegel, S., and S. Milstien. 2011. The outs and the ins of sphingosine-1-phosphate in immunity. *Nat. Rev. Immunol.* **11:** 403–415.

Steinberg, B. E., and S. Grinstein. 2008. Pathogen destruction versus intracellular survival: the role of lipids as phagosomal fate determinants. *J. Clin. Invest.* **118:** 2002–2011.

Sunagawa, S., J. Choi, H. J. Forman, and M. Medina. 2008. Hyperthermic stress-induced increase in the expression of glutamate-cysteine ligase and glutathione levels in the symbiotic sea anemone *Aiptasia pallida*. *Comp. Biochem. Physiol. B Biochem. Mol. Biol.* **151:** 133–138.

Tafesse, F. G., A. Rashidfarrokhi, F. I. Schmidt, E. Freinkman, S. Dougan, M. Dougan, A. Esteban, T. Maruyama, K. Strijbis, and H. L. Ploegh. 2015. Disruption of sphingolipid biosynthesis blocks phagocytosis of *Candida albicans*. *PLoS Pathog.* **11:** e1005188.

Thompson, C. R., S. S. Iyer, N. Melrose, R. VanOosten, K. Johnson, S. M. Pitson, L. M. Obeid, and D. J. Kusner. 2005. Sphingosine kinase

1 (SK1) is recruited to nascent phagosomes in human macrophages: inhibition of SK1 translocation by *Mycobacterium tuberculosis*. *J. Immunol.* **174:** 3551–3561.

Wei, W.-C., P.-J. Sung, C.-Y. Duh, B.-W. Chen, J.-H. Sheu, and N.-S. Yang. 2013. Anti-inflammatory activities of natural products isolated from soft corals of Taiwan between 2008 and 2012. *Mar. Drugs* **11:** 4083–4126.

Weis, V. M., E. A. Verde, A. Pribyl, and J. A. Schwarz. 2002. Aspects of the larval biology of the sea anemones *Anthopleura elegantissima* and *A. artemisia*. *Invertebr. Biol.* **121:** 190–201.

Weis, V. M., S. K. Davy, O. Hoegh-Guldberg, M. Rodriguez-Lanetty, and J. R. Pringle. 2008. Cell biology in model systems as the key to understanding corals. *Trends Ecol. Evol.* **23:** 369–376.

Xia, P., L. Wang, P. A. Moretti, N. Albanese, F. Chai, S. M. Pitson, R. J. D'Andrea, J. R. Gamble, and M. A. Vadas. 2002. Sphingosine kinase interacts with TRAF2 and dissects tumor necrosis factor-α signaling. *J. Biol. Chem.* **277:** 7996–8003.

Yamashiro, H., H. Oku, H. Higa, I. Chinen, and K. Sakai. 1999. Composition of lipids, fatty acids and sterols in Okinawan corals. *Comp. Biochem. Physiol. B Biochem. Mol. Biol.* **122:** 397–407.